X-ray-reflectivity study of the growth kinetics of vapor-deposited silver films

C. Thompson
Physics Department, Polytechnic University, 333 Jay Street, Brooklyn, New York 11201

G. Palasantzas
Physics Department, Northeastern University, Boston, Massachusetts 02115

Y. P. Feng and S. K. Sinha
Exxon Corporate Research Laboratories, Route 22E, Clinton Township, Annandale, New Jersey 08801

J. Krim
Physics Department, Northeastern University, Boston, Massachusetts 02115
(Received 5 August 1993)

X-ray-reflectivity measurements have been carried out on silver films which were vapor deposited onto silicon substrates, to investigate the thickness evolution of the film's surface roughness. The growth exponent was found to be $\beta=0.26\pm0.05$, and the roughness exponenet was found to be $H=0.70\pm0.10$.

I. INTRODUCTION

The technique of x-ray reflectivity is ideally suited to the characterization of nanometer-scale surface roughness, since it involves probing a surface at *microscopic* length scales while sampling a *macroscopic* portion of the surface.[1-5] We report here an x-ray-reflectivity study of the evolution of surface roughness in vapor-deposited films (thermally evaporated silver on silicon), focusing on the overall capabilities of the technique as a probe of thin-film surface roughness, as well as the nonequilibrium growth kinetics of vapor-deposited films. The latter topic has received much recent attention, particularly in the areas of atomic-scale computer simulation and scaling theory,[6] which predict that self-affine fractal surfaces will develop.[7]

All rough surfaces exhibit perpendicular fluctuations which are characterized by a mean-square width $\sigma=\langle z(x,y)^2\rangle^{1/2}$; $z(x,y)=h(x,y)-\langle h(x,y)\rangle$, where $h(x,y)$ is the height function and $\langle\cdots\rangle$ is the spatial average over a planar reference surface. The roughness is termed "Gaussian" if $z(x,y)-z(x',y')$ is a Gaussian random variable whose distribution depends only on the relative coordinates $(X,Y)\equiv(x'-x,y'-y)$. For an isotropic Gaussian rough surface, the mean-square surface fluctuation is $g(R)=\langle[z(x',y')-z(x,y)]^2\rangle$; $R=\sqrt{(X^2+Y^2)}$, where the average is taken over all pairs of points on the surface which are separated horizontally by the length R. The function $G(R)$ is related to the height-height correlation function $C(R)=\langle z(R)z(0)\rangle$ by $g(R)=2\sigma^2-2C(R)$. If the surface exhibits self-affine roughness, $g(R)$ will scale as $g(R)\propto R^{2H}$,[8] where $0<H<1$ is referred to as the "roughness" exponent.[9]

The rms width of a real self-affine surface must saturate at large length scales, so there is a characteristic horizontal cutoff, or correlation length ξ, associated with the surface roughness. For a growing film, the time evolution of the (saturated) rms width is characterized by the "growth" exponent β, where $\sigma\propto t^{\beta}$. (It is generally assumed that the film thickness $\langle h\rangle$ is directly proportional to the deposition time t.)[7] Film growth can alternatively be described in terms of the "dynamic" scaling exponent $z_s=H/\beta$, where the time evolution of the correlation length ξ varies as $\xi\propto t^{(1/z_s)}$. Large-scale computer simulations of nonequilibrium vapor deposition onto two-dimensional substrates[10] suggest that $H\approx0.33$, $\beta\approx0.25$, if no surface diffusion of the deposited film particles occurs upon arrival at the substrate. This scenario is generally referred to as the KPZ model.[11] Alternate models, seeking to incorporate the effects of surface diffusion, yield $H=0.67$, $\beta=0.20$ for deposition onto two-dimensional substrates.[12] These values have not, however, gained universal acceptance, since numerical simulations that include surface diffusion have in some cases yielded the KPZ values, $H\approx0.33$, $\beta\approx0.25$.[13] The values of the scaling exponents, if in fact they are universal,[14] have yet to be thoroughly investigated by experiment. Despite an increasing number of investigations,[15-20] a coherent view has not emerged.

We report here measurement of H and β for the system Ag/silicon by means of x-ray reflectivity, and discuss the overall capabilities of the technique as a probe of thin-film surface roughness. We observe close agreement between the measured exponents and certain theoretical predictions, and examine in detail the consistency between the experimental conditions and theoretical assumptions.

II. EXPERIMENTAL APPARATUS

The x-ray measurements were performed at the National Synchrotron Light Source (NSLS) at Brookhaven National Laboratory, beamline X22C (wavelength $\lambda=1.5377$ Å). Silver films were thermally evaporated *in*

0163-1829/94/49(7)/4902(6)/$06.00

situ onto a silicon substrate mounted within a high-vacuum chamber equipped with beryllium windows. The distance from the center of the sample to the detector was 816 mm, and receiving slit geometry defined a scattering resolution $\Delta\theta \approx 0.012°$. Slit geometry was set for $\approx 1°$ beam acceptance perpendicular to the scattering plane. Scatter slits were used in the beam path to decrease parasitic scattering. The footprint of the sample due to the finite width of the incoming beam corresponded to beam spillover at incident angles of 1.5° or less. Experimental intensities were accordingly adjusted for spillover effects.

The substrate could be rotated by 180° to accommodate either film deposition (downward position), or reflectivity measurements (upward position). Deposition took place at normal incidence and at room temperature onto a 100-mm^2 substrate. The deposition occurred at an average rate of 0.03 nm/s, as measured by a quartz-crystal rate monitor. Data were recorded for five film thicknesses ranging from $\sim 10-150$ nm (as determined by the rate monitor), by halting the evaporation and examining the sample at various stages of film growth.

III. EXPERIMENTAL RESULTS

The scaling exponent β

The specular (angle of incidence equal to angle of reflection) reflection of x-rays from surfaces yields information about the rms surface width and also the film-density distribution.[1-5] Such measurements involve recording the scattered intensity as a function of $q_z = 4\pi/\lambda \sin(\theta)$, where q_z is the wave-vector transfer perpendicular to the surface. Specular-reflectivity data for the five silver film thicknesses, corrected for background and beam spillover at low angles, are displayed in Figure 1(a). Oscillations in the data arise from interference between the portion of the beam reflected from the silver-vacuum interface (i.e., the silver-film surface) and that reflected from the silicon-silver interface. The increasing rate at which successive curves decay is primarily due to the increasing width of the silver-vacuum interface.

The specular reflectivity data were fit (Fig. 1(b), solid lines) using a standard analysis approach based on a homogeneous stratified layer,[4,21,22] where layer thickness, interfacial (Gaussian) widths (σ), and densities associated with each layer were the fitting parameters. The scaling exponent β was obtained from the thickness dependence of the width determined for the silver-vacuum interface (Fig. 1(b), inset), $\sigma \propto t^{\beta}$. The solid line in the Fig. 1(b) inset has slope $\beta = 0.26 \pm 0.05$. Each value of σ presented in Fig. 1(b) has been corrected for the rms width of the silicon substrate σ_s, according to the relation $\sigma_c = \sqrt{\sigma^2 - \sigma_s^2}$. This correction alters the value of β by less than 0.02.

The scaling exponent H

The diffuse (angle of incidence not equal to the angle of reflection) component of the scattering is related to height-height correlations of the rough surface. Sinha *et al.*[23] used perturbation theory on the exact solution of the wave equation for a smooth surface to calculate the diffuse scattering produced by surface roughness. The data presented here were recorded, as is typically the case,[15,24,25] with a slit instead of a pinhole geometry, so that the Ref. 23 expressions for the diffuse scattering, integrated over the acceptance perpendicular to the scattering plane, are given as

$$I(q_x,q_z) = I_0 \frac{\Delta\Omega}{A}(L_x L_y)\frac{|k_0^2(1-n^2)|^2}{16\pi^2} \times |T(\mathbf{k}_1)|^2 |T(\mathbf{k}_2)|^2 S(q_x) , \quad (1a)$$

$$S(q_x,q_z) = \frac{\exp(-[(q_z^2)^2 + (q_z^{t*})^2]\sigma^2/2)}{|q_z^t|^2} \times \int_0^{\infty} (e^{|q_z^t|^2 C(X)} - 1)\cos(q_x X)\,dX . \quad (1b)$$

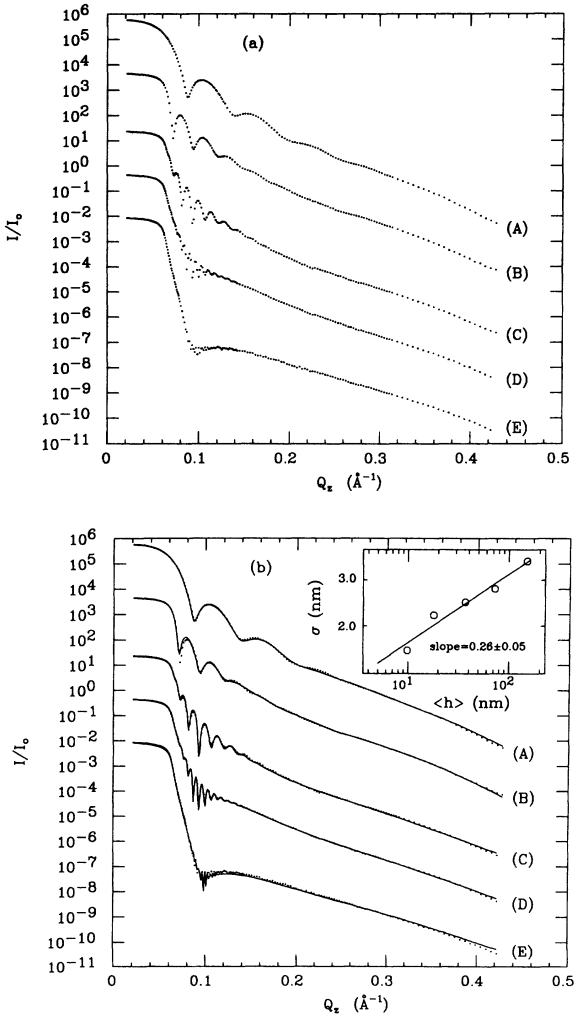

FIG. 1. (a) Specular-reflectivity data for progressively thicker Ag films. (A) 9.8 nm, (B) 18 nm, (C) 36.7 nm, (D) 72.8 nm, (E) 150.2 nm. (b) Fits (solid lines) to the specular-reflectivity data. The inset depicts a log-log plot of σ vs film thickness, with slope $\beta = 0.26 \pm 0.05$.

The terms $\mathbf{k}_1$ and ($\mathbf{k}_2$) are the incident and reflected wave vectors, k_0 the wave-vector magnitude, q_x and q_z^t the in-plane x component and in-medium z component of the wave-vector transfer, $T(\mathbf{k})$ the Fresnel transmission coefficient, n the index of refraction, L_xL_y the area illuminated by the beam, I_0 and A the intensity and cross-sectional area of the beam, and $\Delta\Omega$ the solid angle subtended by the detector at the sample.

The diffuse cross section (recorded at specular condition) of a self-affine surface with no cutoff [Eqs. (1) with $\xi=\infty$ and $q_x=0$] has the asymptotic form

$$I(q_z)\propto(L_xL_y)\sigma^{-2/H}q_z^{-[2+(1/H)]}. \tag{2}$$

If the area illuminated by the beam changes as the diffuse data are recorded, then $(L_xL_y)\propto q_z^{-1}$ and the experimentally observed power law will have the form

$$I(q_z)\propto\sigma^{-2/H}q_z^{-(3+1/H)}. \tag{3}$$

Numerical calculations reveal this asymptotic form to hold also when the horizontal cutoff is taken into account.[26]

A plot of the diffuse intensity at specular condition versus q_z can only in principle provide an experimental measure of the parameter H. Since there are both specular and diffuse contributions to the scattering intensity recorded at specular condition, the sample must be offset slightly from the specular condition to remove the specular component. If the incident angle is θ_1, then the intensity is measured at an angle $\theta_2=\theta_1\pm\varepsilon$ where $\varepsilon\ll 0_1$, but large enough to eliminate the specular contribution.

Figure 2 displays "off-specular" diffuse reflectivity data plotted versus q_z on a log-log scale for the five film thicknesses. The data have been recorded with the sample offset from the specular condition by $+0.05°$. They have been adjusted for spillover effects in a manner which renders Eq. (3) the applicable asymptotic form. Corrections for the scintillation counter "dark count" and

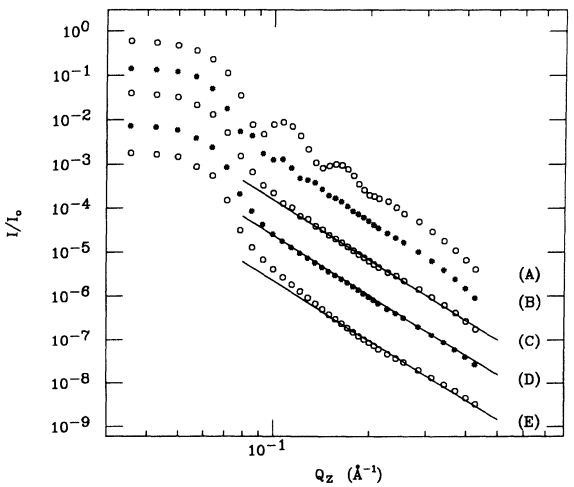

FIG. 2. Diffuse background reflectivity data for progressively thicker Ag films. (A) 9.8 nm, (b) 18 nm, (C) 36.7 nm, (D) 72.8 nm, (E) 150.2 nm. The data were recorded at a $+0.05°$ offset from the specular condition. Linear fits to the diffuse data for thicknesses (C)–(E) correspond to $H=0.63$ for a single-interface model.

parasitic scattering are neglected. According to Eq. (3), these plots will be straight lines with slope $-(3+1/H)$ if the surface is self-affine. Diffuse scattering from a lower interface that is not correlated to that of the upper interface will add (as a scalar) to that reflected from the upper interface. Taking note of the prefactor $\sigma^{-2/H}$ in Eqs. (2) and (3), and the fact that σ_s for the lower interface is much smaller than that of the upper interface, it can be seen that diffuse contributions from the lower interface become negligible as the rms width of the upper interface increases. Interference effects, which arise on account of correlations in the roughness between the surface and the interface, must be accounted for whenever they are substantial enough to produce oscillations in the data. Equation (3) cannot be applicable to the first two thicknesses (curves A,B) on account of oscillations in the data, but linear portions of the data are present for the third, fourth and fifth thicknesses (curves C,D,E). The value $H=0.63\pm0.05$ is obtained from the best fit to these linear portions for $q_z\sigma>1$.

In order to gauge the accuracy of the value of H determined via this simple, single-interface analysis, as well as the underlying assumption of a Gaussian roughness distribution, we examined correlation data from scanning-tunneling-microscope (STM) images recorded on silver films prepared in the identical vacuum chamber (Fig. 3). Eight 600×600 nm^2 images were recorded on a 73-nm-thick sample in a dry N_2 environment with a commercial (Digital Instruments Nanoscope II) STM, with a grid density of 400 lines by 400 points per line. Height-height correlations were computed directly from the data sets after the ensemble average was performed. The roughness exponent was obtained from the dependence of $g(R)$ at small R, $g(R)\propto R^{2H}$, yielding $H=0.78\pm0.014$. The value $\sigma=3.2$ nm was the average standard height deviation for the topographs. The data are reasonably described by the analytic form $g(R)=2\sigma^2\{1-\exp[-(R/\xi)^{2H}]\}$,[27] with $H=0.78$, $\sigma=3.2$ nm, and $\xi=23.0$ nm (Fig. 3, solid line). Various other analytic forms for $g(R)$, as well as the present form, are discussed in great detail in Ref. 26.

The physical significance of ξ can be observed in the STM image, where it is on the order of the largest cluster size, as well as in the correlation data, where it is located at a point where significant deviations from power-law behavior are observed. We note that the sample studied here was well described by a simple Gaussian height distribution (Fig. 3, inset plot).

The value of H determined from the STM data is greater than that determined from the simple, single-interface analysis of the x-ray data. Comparison of the x-ray data to theoretical profiles generated by means of a two-interface formalism[28] demonstrated the most probable range for the roughness exponent to be (assuming no knowledge of the STM data) $0.65<H<0.75$. We note that the value $H=0.63$ obtained from the simple, single-interface analysis is essentially the lower limit to the range of all permissible values established by the two-interface formalism. Extensive efforts involving the development of a multiple interface formalism are in progress.[29]

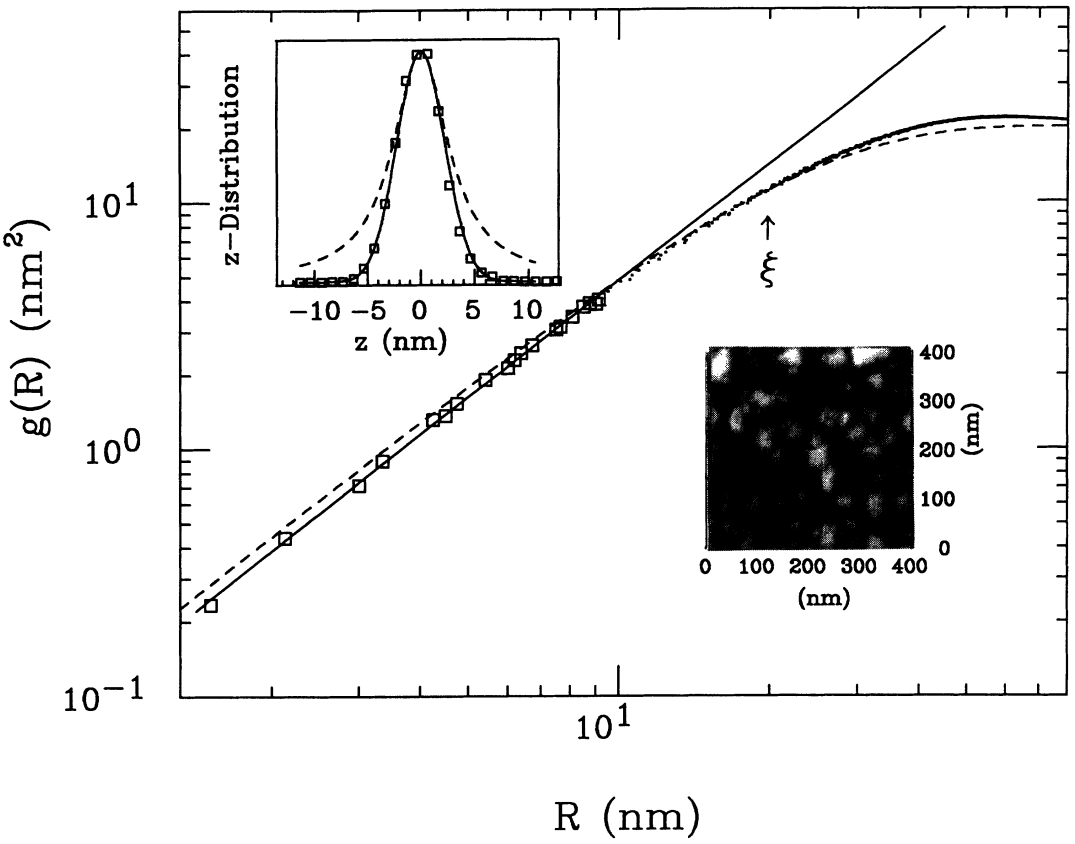

FIG. 3. Height-difference correlation data obtained from STM images recorded on a 73-nm-thick silver film. The solid line is a fit to those data points represented by squares, and has slope $2H$, with $H=0.78\pm0.014$. The dashed line depicts the function $g(R)=2\sigma^2[1-e^{(R/\xi)^{2H}}]$ with $H=0.78$, $\xi=23$ nm, and $\sigma=3.17$ nm. The upper inset displays best fits of the surface height distribution (squares) to Gaussian $\propto e^{-(z/\sigma)^2}$ (solid line), and Lorentzian $\propto[(z^2+\sigma^2)^{-1}]$ (dashed line) distribution functions. The lower inset displays a typical STM image for this sample. The height scale (black to white) is 0–31 nm.

The scaling exponent $z_s=H/\beta$

The values $\beta=0.26$ and $H=0.70$ ($H=0.70$ is the average of the range $0.60<H<0.80$ established by the x-ray and STM analyses) correspond to a dynamic scaling exponent $z_s=H/\beta=2.7$. The correlation length should therefore scale with film thickness as $\xi\propto\langle h\rangle^{\frac{1}{2.7}}$. This relation can be investiagated independently by examining the diffuse scattering component of a rocking-curve scan. In this geometry, the detector is held at a fixed angle, and the sample is rocked about the specular condition. A central maximum in the intensity I_s for such a scan corresponds to the specular condition $\theta_1=\theta_2$. The scattering profile also has intensity peaks I_ω at the critical angle θ_c for total external reflection, θ_1, $\theta_2=\theta_c$. The diffuse region outside of the central maximum can be fit to Eq. (1) to yield an experimental value for the correlation length.

Figure 4 displays rocking-curve data for the five film thicknesses. The upper curve in each plot represents the recorded data, while the lower curve represents the data corrected for contributions that arise from scattering off of the silicon-silver interface. Corrections were carried out under the assumption that the scattering from each interface was not correlated, since the data were recorded at $2\theta=4.0°$, or $q_z=0.28$ Å^{-1}, where oscillations are absent in both the off-specular and rocking-curve diffuse data. The silicon-silver contribution was calculated by first enhancing the data recorded for the bare silicon substrate by a factor reflecting the increased electron density contrast for the silicon-silver interface over that of silicon vacuum. This enhanced data was then adjusted for the attenuation of the beam on account of its path through the silver film.

The corrections are substantial enough to render the data sets nearly flat in the diffuse region where fits are normally performed. The data are, however, consistent with curves generated from the Eq. (1) expressions (solid lines in Fig. 4), employing the experimentally determined values for H and β, which imply a thickness dependence for ξ of

$$\xi=19.9\langle h\rangle^{1/2.7}\ \text{Å}\ . \tag{4}$$

In order to have obtained reliable fits to data recorded on this sample and at these scattering conditions, the correlation lengths would have to have exceeded ≈100 nm, for roughness exponents in the range $0.60<H<0.80$.

Summary

Our central results are summarized as follows

(i) Precise values for σ can, in general, be obtained from fits to specular-reflectivity data recorded on thin

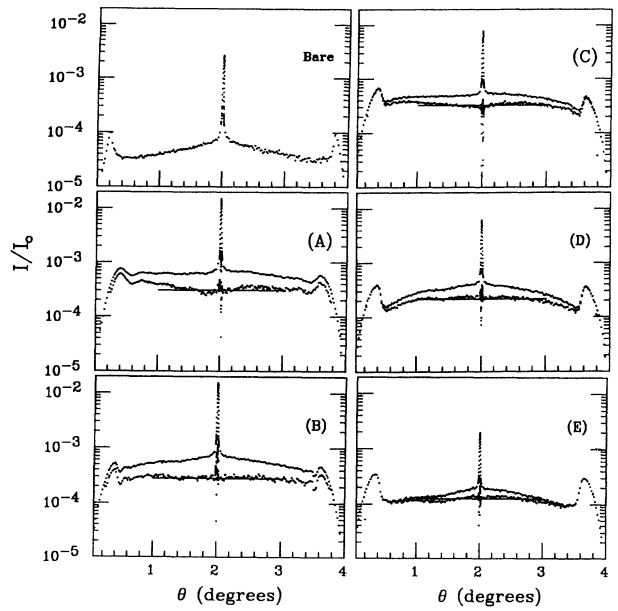

FIG. 4. Rocking-curve data for the bare substrate and the five film thicknesses: (A) 9.8 nm, (B) 18 nm, (C) 36.7 nm, (D) 72.8 nm, (E) 150.2 nm. Solid lines represent theoretically generated curves with correlation lengths taken from Eq. (4). The upper data set in each plot are the recorded data, and the lower set shows the data after correcting for the substrate contribution.

film samples by means of a homogeneous stratified layer theory. This allows for precise determination of the growth exponent β. For the case at hand, we observe $\beta=0.26\pm0.05$.

(ii) The asymptotic behavior of off-specular diffuse reflectivity data provides a direct means for determining the roughness exponent H [Eqs. (2) and (3)] for a single interface. For a thin-film sample, diffuse scattering from the lower interface(s) may alter this result, but the single-interface analysis appears to establish a lower bound for the true value of H. For the case at hand, we observe $H=0.70\pm0.10$.

(iii) Diffuse rocking-curve data provide a means to determine ξ, allowing an independent measure of the dynamic scaling exponent z_s. For the case at hand, the film correlation lengths were not large enough to allow for precise determination of ξ and z_s. The rocking-curve data are, however, consistent with the values of ξ and z_s that were determined from the STM, specular-, and off-specular-reflectivity-data analyses.

(iv) The samples studied here were well described by a simple Gaussian roughness distribution.

IV. DISCUSSION

The values we report here coincide with those reported by Chevrier *et al.*[17] ($\beta=0.25-0.32$), and He, Yang, and Lu[18] ($H=0.79\pm0.05$; $\beta=0.22\pm0.02$) for vapor-deposited iron films. They do not coincide with the values reported by Chiarello *et al.*[15] ($H\approx0.50$) and You *et al.*[20] ($H=0.42$, $\beta=0.40$) for vapor-deposited silver and gold films. We attribute the difference with the result of Chiarello *et al.* to the lower substrate temperature (associated with limitations on surface diffusion) employed for that study. We attribute the difference with the result of You *et al.* to either a difference in film deposition conditions or to their analysis approach. Eklund *et al.*[16] and Krim *et al.*,[19] respectively, reported $H=0.2-0.4$ and $H=0.52\pm0.02$ for room-temperature studies of iron-film erosion. In principle, their results should be comparable to vapor-deposition models, but the argument has not been conclusively established. We note that x-ray reflectivity would be a particularly powerful technique for erosion studies, since multiple-interface complications would be absent, and the correlation lengths are expected to be larger.[19]

The values $H=0.70\pm0.10$ and $\beta=0.26\pm0.05$ that we have measured are close to those obtained from the model of Villain, Das Sarma, and others, $H=0.67$, $\beta=0.20$. Since the substrate temperature is relatively high, surface-diffusion effects are expected to be important in this system. Indeed, since the films are not electrically conductive below ~10 nm on account of cluster formation, surface-diffusion effects must, in fact, be present. Additional consistencies between theory and experiment include the silver-film densities (which are observed to be quite close to that of bulk silver), and the sticking coefficient of the incoming silver atoms (which is close to unity). We note that although the experimental value for H is not consistent with the KPZ value, the value obtained for β is within experimental error of the KPZ value.

One significant discrepancy between the experimental conditions and all of the deposition models is that grain boundaries are not included in the modeling. A standard theoretical assumption is that deposition occurs on a perfectly flat substrate, with no mechanism included to account for the formation of the polycrystalline grains after the growth commences. Such grains certainly occur in the present experiment, and are to be expected for the majority of vapor-deposited films. In order for nonequilibrium growth models to be more physically realistic, it would be interesting to examine growth on the surface of crystallites, that are misoriented with respect to each other. Further experimental studies will also be required to address the actual importance of this issue in determining the scaling behavior of the deposited films. For example, it would be desirable to repeat the present experiment by studying film growth on a silver single-crystal surface rather than a silicon surface. This would reduce the effect, if any, of grain boundaries. At present, we conclude that the theory and experiment are suggestively close, notwithstanding the fact that the conditions assumed by the theory are not in perfect harmony with those of the experiment.

ACKNOWLEDGMENTS

This work was supported in part by NSF Grant Nos. DMR-8657211, DMR-9204022 (J.K. and G.P.). R. M. Suter is thanked for a careful reading of the manuscript. J. Villain and D. Wolf are thanked for enlightening discussions.

[1]S. K. Sinha, E. B. Sirota, S. Garoff, and H. B. Stanley, Phys. Rev. B **38**, 2297 (1988).
[2]A. Braslau, P. S. Pershan, G. Swislow, and B. M. Ocko, Phys. Rev. A **38**, 2457 (1988).
[3]P. Z. Wong and A. Bray, Phys. Rev. B **37**, 7751 (1989).
[4]M. F. Toney and C. Thompson, J. Chem. Phys. **92**, 3781 (1990).
[5]J. D. Shindler and R. M. Suter, Rev. Sci. Instrum. **63**, 5343 (1992).
[6]For a recent review, see *Surface Disordering: Growth, Roughening and Phase Transitions,* edited by R. Jullien, J. Kertesz, P. Meakin, and D. E. Wolf (Nova Science, Commack, 1992).
[7]F. Family and T. Vicsek, J. Phys. A **18**, L75 (1985).
[8]F. Family and T. Vicsek, *Dynamics of Fractal Surfaces* (World Scientific, Singapore, 1991).
[9]J. Krim and J. O. Indekeu, Phys. Rev. E **48**, 1579 (1993).
[10]P. Meakin, P. Ramandal, L. M. Sander, and R. C. Ball, Phys. Rev. A **34**, 5091 (1986).
[11]M. Kardar, G. Parisi, and Y. Zang, Phys. Rev. Lett. **56**, 889 (1986).
[12]D. E. Wolf and J. Villain, Europhys. Lett. **13**, 389 (1990); Z.-W. Lai and S. Das Sarma, Phys. Rev. Lett. **66**, 2348 (1991).
[13]H. Yan, Phys. Rev. Lett. **68**, 3048, (1992); D. A. Kessler, H. Levine, and L. M. Sander, *ibid.* **69**, 100 (1992).
[14]Y.-C. Zhang, J. Phys. **51**, 2129 (1990).
[15]R. Chiarello, V. Panella, J. Krim, and C. Thompson, Phys. Rev. Lett. **67**, 3408 (1991).
[16]E. A. Eklund, R. Brouinsma, J. Rudnick, and R. S. Williams, Phys. Rev. Lett. **67**, 1759 (1991).
[17]J. Chevrier, V. Le Thanh, R. Buys, and J. Derrien, Europhys. Lett. **16**, 737 (1991).
[18]Y.-L. He, H.-N. Yang, and T.-M. Lu, Phys. Rev. Lett. **69**, 3770 (1992).
[19]J. Krim, I. Heyvaert, C. V. Haesendonck, and Y. Bruynseraede, Phys. Rev. Lett. **70**, 57 (1993).
[20]H. You, R. P. Chiarello, H. K. Kim, and K. G. Vandevoort, Phys. Rev. Lett. **70**, 2900 (1993).
[21]M. Born and E. Wolf, *Principle of Optics* (Pergamon, Oxford, 1970).
[22]J. Als.-Nielsen, in *Handbook on Synchrotron Radiation* (North-Holland, New York, 1991), Vol. 3.
[23]See Eqs. (4.41) and (4.42) of Ref. 1.
[24]D. E. Savage *et al.*, J. Appl. Phys. **69**, 1411 (1991).
[25]W. Weber and B. Lengler, Phys. Rev. B **46**, 7953 (1992).
[26]G. Palasantzas and J. Krim, Phys. Rev. B **48**, 2873 (1993).
[27]See Eq. (29) of Ref. 1.
[28]R. Pynn, Phys. Rev. B **45**, 602 (1992).
[29]S. K. Sinha *et al.* (unpublished).

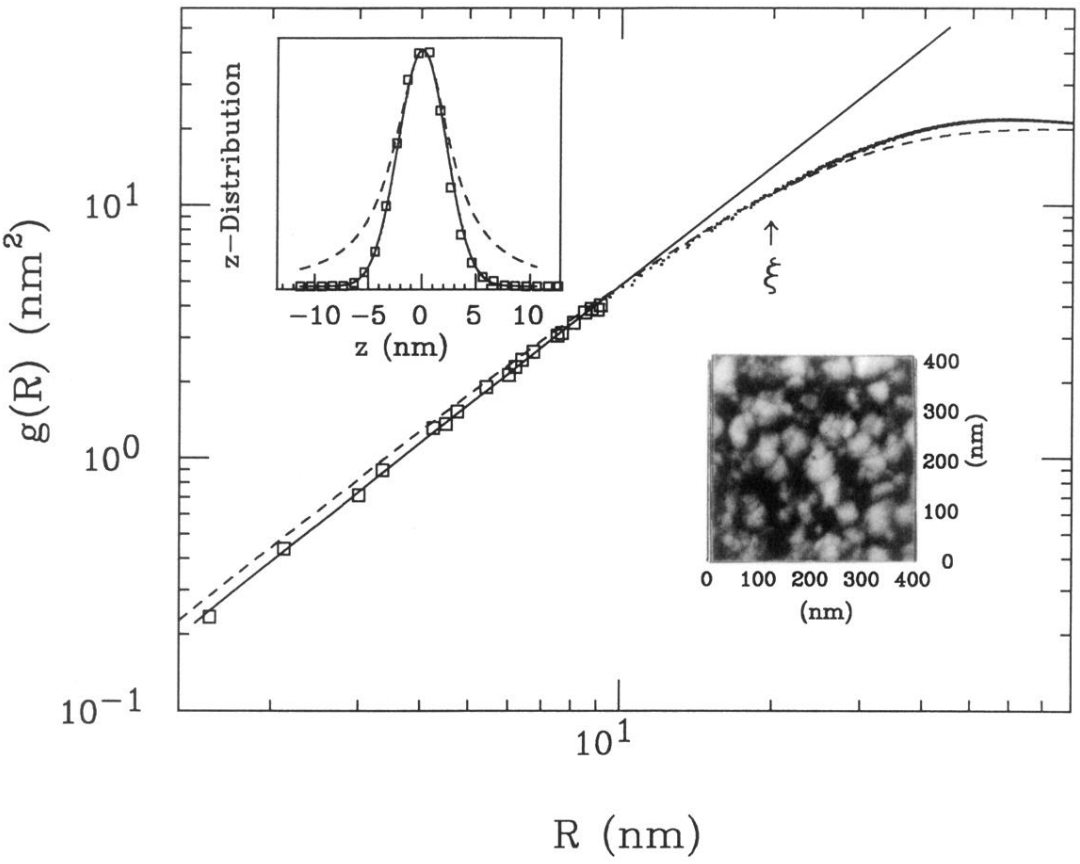

FIG. 3. Height-difference correlation data obtained from STM images recorded on a 73-nm-thick silver film. The solid line is a fit to those data points represented by squares, and has slope $2H$, with $H=0.78\pm0.014$. The dashed line depicts the function $g(R)=2\sigma^2[1-e^{(R/\xi)^{2H}}]$ with $H=0.78$, $\xi=23$ nm, and $\sigma=3.17$ nm. The upper inset displays best fits of the surface height distribution (squares) to Gaussian $\propto e^{-(z/\sigma)^2}$ (solid line), and Lorentzian $\propto[(z^2+\sigma^2)^{-1}]$ (dashed line) distribution functions. The lower inset displays a typical STM image for this sample. The height scale (black to white) is 0–31 nm.